SOILS AND FOUNDATIONS Vol. 32, No. 1, 59-70, Mar. 1992
Japanese Society of Soil Mechanics and Foundation Engineering

FINITE ELEMENT SLOPE STABILITY ANALYSIS BY SHEAR STRENGTH REDUCTION TECHNIQUE

TAMOTSU MATSUI[i] and KA-CHING SAN[ii]

ABSTRACT

A shear strength reduction technique for finite element slope stabilityan alysis has been developed by the authors. An important orginal point in the proposed method is that the slope failure is defined according to the shear strain failure criterion. The aim of this paper is to verify the shear strength reduction technique for the finite element slope stability analysis. Are presented the detailed background behind the shear strength reduction technique, the elucidation of the physical meaning of the critical shear strength reduction ratio in regard to the total shear strain and shear strain increment for both embankment and excavation slopes and its practical application to a field test on a reinforced slope cutting.

As the results, the critical shear strength reduction ratio agrees with the safety factor by the Bishop's method if total shear strain is used for analyses of embankment slopes. In the case of the natural excavation slopes, in which total shear strain is difficult to be assessed, the safety factor can be related to the average of the local safety factors along the failure slip surface obtained by the shear strength reduction technique. The predicted behavior of the reinforced slope cutting agrees with the field test data and site observation. Agreement between the shear strength reduction technique and a modified Fellenius' method is satisfactory. Consequently, applicability of the proposed method to practical design works is demonstrated.

Key words : failure, finite element method, safety factor, slip surface, slope stability, stability analysis (**I. G. C** : E 6)

INTRODUCTION

The principle behind the shear strength reduction technique, which has previously been proposed by the authors (Matsui and San, 1988), in the finite element slope stability analysis is to reduce c and $\tan\phi$ until slope failure occurs, in which the failure of slope is defined as that the failure shear strain develops from the toe to the top of the slope. The technique has been applied to two practical reinforced cut slope projects-the Kashiwara site and the Nose site (Matsui and San, 1989 a, 1990 a). Examples of its application to other problems were also reported by other research workers (e. g. Ugai, 1990). The potential of the use of the shear strength reduction technique to

i) Professor, Department of Civil Engineering, Osaka University, Osaka.
ii) Research Associate, Department of Civil Engineering, Osaka University, Osaka.
Manuscript was received for review on June 29, 1990.
Written discussions on this paper should be submitted before October 1, 1992, to the Japanese Society of Soil Mechanics and Foundation Engineering, Sugayama Bldg. 4 F, Kanda Awaji-cho 2-23, Chiyodaku, Tokyo 101, Japan. Upon request the closing date may be extended one month.

the finite element slope stablity analysis in practice seems to be recognized.

In our previous paper (Matsui and San, 1990 b), by using the shear strength reduction technique, a hybrid slope stability analysis method for cut slope was proposed and the result of its application to the field test in the Kashiwara site was presented. However, the physical meaning of the critical shear strength reduction ratio was not yet elucidated.

This paper presents verification of the shear strength reduction technique to the finite element slope stability analysis. First, the detailed backgroun dbehind the shear strength reduction technique is presented. Next, in regard to the total shear strain and shear strain increment, the relationship between the critical shear strength reduction ratio and the safety factor for both embankment and excavation slopes is discussed. Then, the verification of the shear strength reduction technique through the field test data in the Nose site is presented. Finally, for the reinforced slope cutting in the Nose site, stability analysis results by the shear strength reduction technique are compared with those by a modified Fellenius' method.

THE SHEAR STRENGTH REDUCTION TECHNIQUE

In the finite element analysis, it is difficult to trace the failure slip surface of a slope, being based on the stress failure criterion. Alternatively, the shear strain failure criterion is employed herein.

Many laboratory test results have shown that the failure shear strain zone coincided with the rupture surface (e. g. Roscoe, 1970). Therefore, it is assumed that the failure mechanism of slope is directly related to the development of the shear strain in the shear strength reduction technique. Also, the existence of the shear strength dependency of the strain is assumed. As the stability of slope is a function of the shear strength and the developement of failure shear strain reflects the potential failure

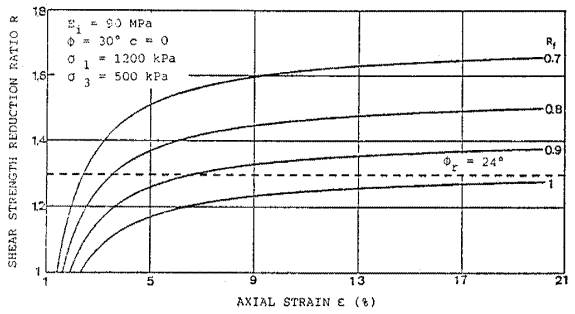

Fig. 1. R versus ε

zone of slope, the shear strain developed in the slope increases with reducing the shear strength. In the following, the form of the shear strength dependency of the strain exhibited in a hyperbolic stress and strain model will be examined.

The hyperbolic stress-strain relationship (Duncan and Chang, 1970) is expressed as

$$\varepsilon=\frac{\sigma_1-\sigma_3}{E_i\left[1-\dfrac{R_f(\sigma_1-\sigma_3)(1-\sin\phi_r)}{(2c_r\cos\phi_r+2\sigma_3\sin\phi_r)}\right]} \quad (1)$$

where ε is the axial strain, σ_1 the major principal stress, σ_3 the minor principal stress, R_f the failure ratio, E_i the initial tangent modulus, c_r and ϕ_r the reduced shear strength parameters, which are defined as

$$c_r=\frac{c}{R},\quad \tan\phi_r=\frac{\tan\phi}{R} \quad (2)$$

where c and ϕ are the shear strength parameters, R the shear strength reduction ratio.

Fig. 1 shows an example of the relationship between the shear strength reduction ratio R and axial strain ε, for different values of R_f. From Fig. 1, it can be seen that the value of ε increases as the value of R increases, especially it increases rapidly when the value of R approaches a certain critical value, which varies with the value of R_f. For the case of $R_f=1.0$, the critical value of R is about 1.3, i. e. the critical value of ϕ_r is about 24° in this example. The critical value of R increases with reducing the value of R_f.

In the following chapter, numerical examples of the application of the shear strength reduction technique to embankment and excavation slopes will be given. The hyper-

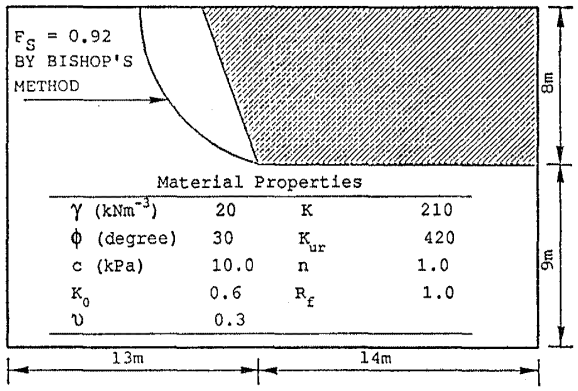

Fig. 2. The slope to be analyzed

bolic nonlinear elastic soil model is used in this paper for practical purpose. It should be noted that the shear strength reduction technique can be applied with other soil models, such as elastoplastic models (e. g. San and Matsui, 1991).

RELATIONSHIP BETWEEN THE CRITICAL SHEAR STRENGTH REDUCTION RATIO AND THE SAFETY FACTOR

In this chapter, the relationship between the critical shear strength reduction ratio and the safety factor will be analytically examined to elucidate their physical meaning. Fig. 2 shows a 70° slope with height of 8 m. The material properties of the ground together with the failure slip surface of the slope by Bishop's method are also given in Fig. 2.

The finite element analysis of the embankment slope was performed by adding elements from the bottom to the top of the slope, and applying the gravity force to each element. For the excavation problem, the analysis was performed by removing the elements from the top to the bottom of the shaded area shown in Fig. 2 to simulate the excavation sequence.

Fig. 3 shows the developments of total shear strain in the embankment for different values of R. The analysis started with R= 0.95 and the value of R was gradually increased, i. e. the shear strength was reduced. As R increases to 0.97, a well defined failure shear zone, in which the shear strains exceed 15%, is developed from the toe to the top of the embankment. The critical value of the shear strength reduction ratio (R_c=

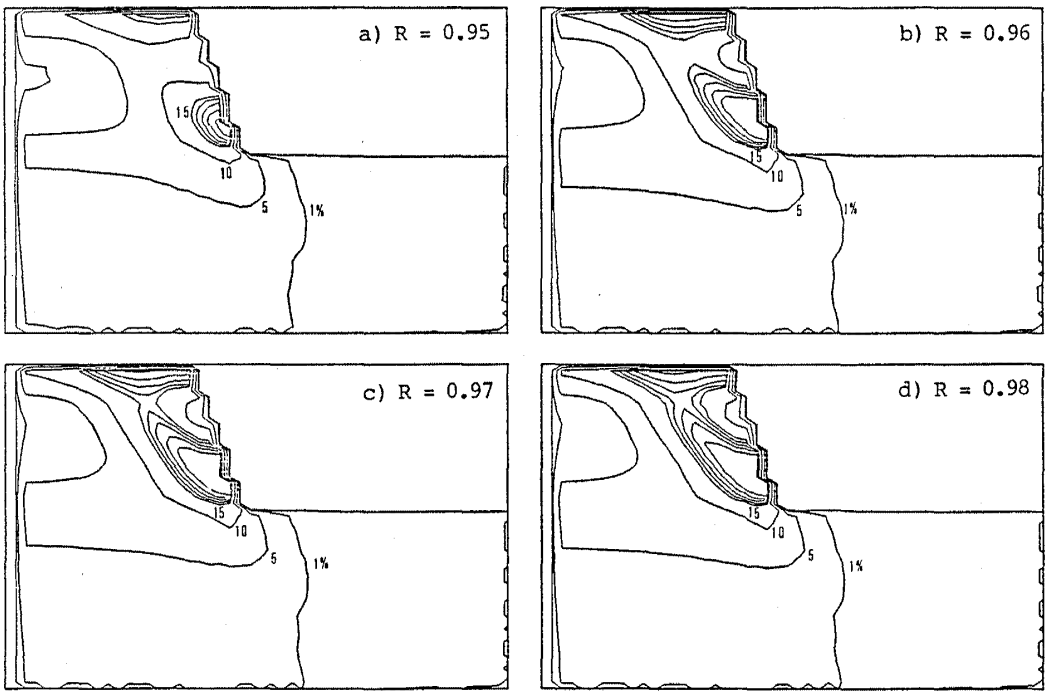

Fig. 3. Total shear strain distributions of the embankment slope with different values of R

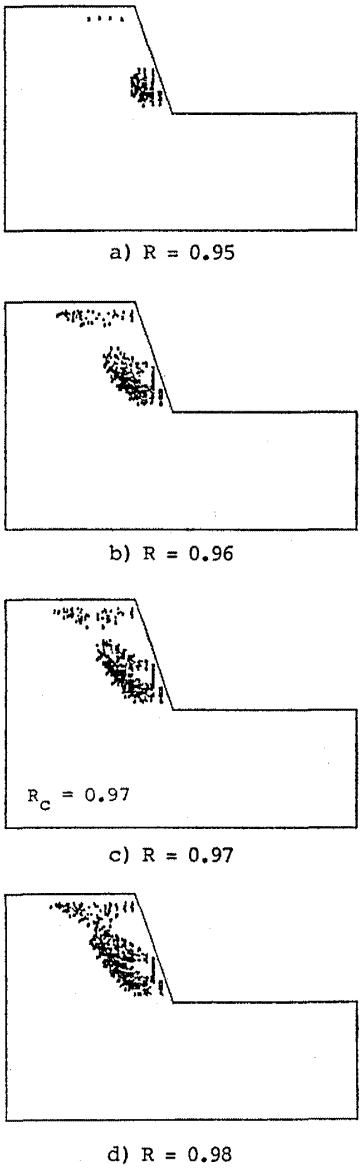

Fig. 4. Failure patterns of the embankment slope with different values of R

0.97) approximately agrees with the safety factor (F_s=0.92) by the Bishop's method. The failure pattern of the embankment can be traced from the location of the shear strains exceeding the failure value. Fig. 4 shows the failure patterns of the embankment slope for the different values of R. The dotted pattern shown in Fig. 4 represents the shear strain exceeding 15%. From this figure, it can be seen that the failure pattern of the embankment for the case of $R=R_c$ is close to the failure slip surface by the Bishop's method. It should be noted that the value of R_c of the slope increases with reducing the value of R_f, which has been presented in elsewhere (San, Matsui and Katsuraya, 1990). For this example, R_c=1.04 as R_f=0.9 and R_c=1.18 as R_f=0.8. The value of R_f can be evaluated from trixial test results. The effect of R_f on the critical value of shear strength reduction ratio has been discussed in the previous chapter. The results of the slope stability analysis agree with the trend in Fig. 1, which is obtained from Eqs. (1) and (2).

Fig. 5 shows the developments of the shear strain increment for different values of R in the excavation slope. Due to the uncertainty of the initial shear strains in the excavation slope before excavation, only shear strain increment development under the effect of excavation is considered. The shear strain increment increases as the value of R increases. Unlike the case of embankment slope, a well defined failure shear strain zone is not formed in the excavation slope, because some contours are not concentrated within a narrow zone, as shown in Fig. 5. However, the contour of the 5% shear strain increment in Fig. 5(d) is very similar to the failure slip surface by the Bishop's method, (see Fig. 2). The dotted patterns shown in Figs. 6(a), (b), (c) and (d), represent that the shear strain increments just exceed the 3%, 4%, 5% and 6% failure shear strains, respectively. It can be seen from this figure that the critical value of R depends on the assumed failure shear strain γ_f. In order to overcome this shortcoming, a hybrid method for cut slope has been proposed (Matsui and San, 1990b), that is, the safety factor is calculated from the stress level at R=1.0, once the slip surface is traced at $R=R_c$. It should be noted that, in spite of the significant variation of R_c and γ_f, the failure patterns of the slope do not change so much, as shown in Fig. 6. For example, the value of failure shear strain is assumed to be 5%. The average value F_S of the local safety factors along the slip surface of the excavation slope is 1.07, which is a little bit greater than the safety factor by the Bishop's method. The

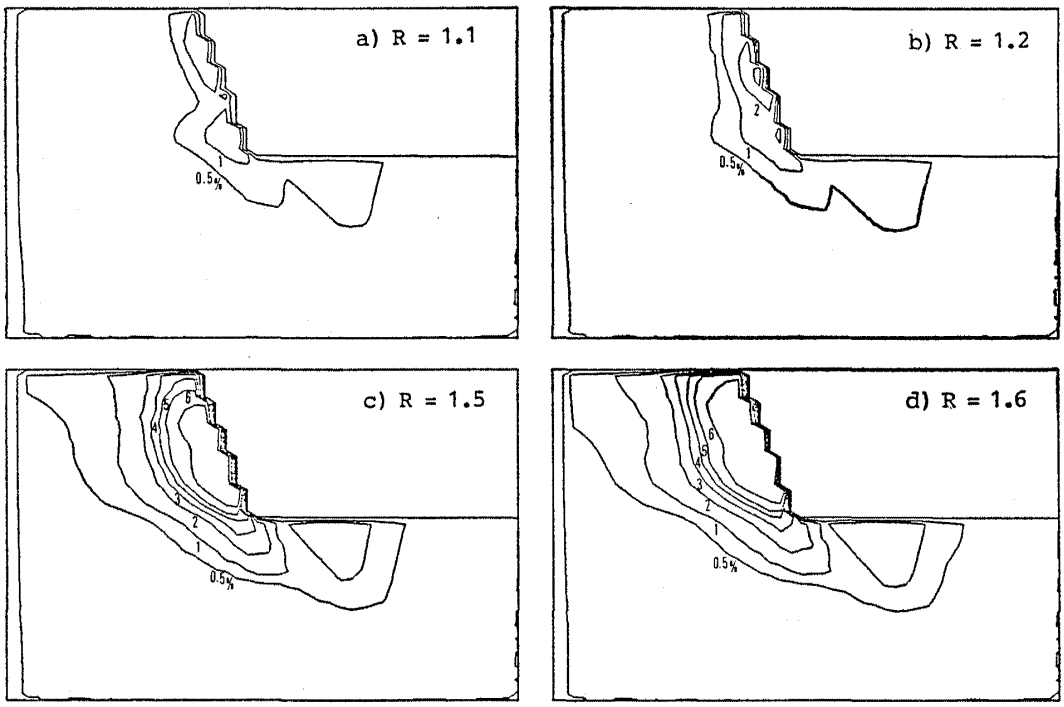

Fig. 5. Shear strain increment distributions of the excavation slope with different values of R

variation of F_S and the failure pattern of the excavation slope for different values of K_0 has been discussed in elsewhere (San, Matsui and Katsuraya, 1990). It has been shown that the failure pattern affects by the value of K_o, and F_S increases as the value of K_o increases.

Fig. 7 shows the comparison between the development of total shear strain in the embankment slope and that of shear strain increment in the excavation slope during construction at $R=R_c$. As shown in Fig. 7 (a), the failure shear strain zone of the embankment slope can be directly postulated from the development of total shear strain, therefore, R_c corresponds to F_S. As shown in Fig. 7(b), a failure shear zone cannot be obtained from the development of shear strain increment, therefore, R_c cannot be used as F_S.

From these analytical results, it can be concluded that the failure patterns of embankment and excavation slopes can be successfully traced by using the shear strength reduction technique. R_c corresponds to F_S if the total shear strain is used in the analysis, for example in the embankment slope. Due to the uncertainty of the initial shear strain condition of the natural slope, only the shear strain increment is available for cases of the excavation slope. Consequently, R_c cannot be used as the safety factor of the excavation slope. However, the safety factor of the excavation slope can be caluculated from the local safety factors along the failure slip surface which can be traced by the shear strength reduction technique. The effects of the stress and strain relationship and the K_o value on the slope stability analysis have been also discussed in elsewhere (San, Matsui and Katsuraya, 1990). Such effects seem difficult to be represented in the limit equilibrium method.

VERIFICATION OF THE SHEAR STRENGTH REDUCTION TECHNIQUE THROUGH THE FIELD TEST DATA

In this chapter, the verification of the shear strength reduction technique through the data of a full-scale field excavation test on a reinforced slope in the Nose site will

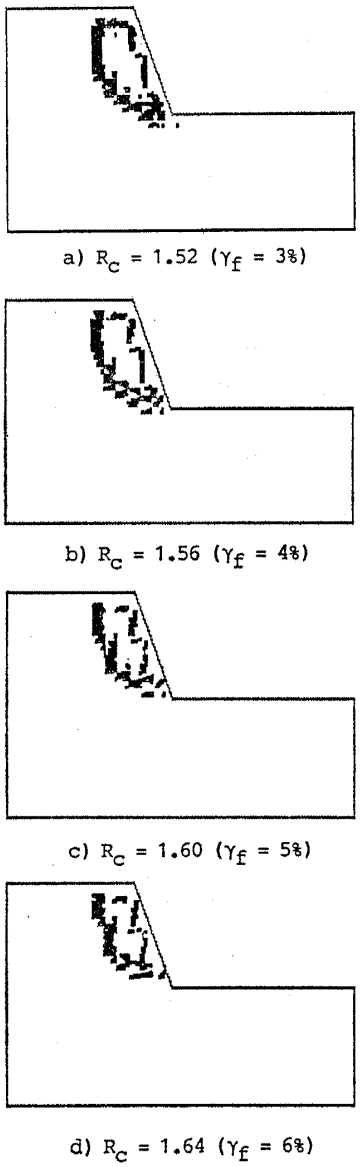

Fig. 6. Failure shear strain patterns of the excavation slope with different values of R_c

be presented. The details of the test site and the field test was reported elsewhere (Matsui and San, 1990 a). Fig. 8 shows the axial force distributions of reinforcements at just after excavation completion and one month later, obtained from the field test. The axial forces increase as the time after excavation elapses. The maximum tensile force locates around the interface between the soil and the soft rock.

The automatic mesh generation was employed in the analysis. It consisted of such four steps as making contours of the ground, arranging of the reinforcements, forming super element mesh and generating finite element mesh, as shown in Fig. 9.

The original ground was assumed as horizontal. The excavation was divided into three parts. The first excavation simulated an erosion process to form the natural slope, the second part of excavation the actual construction sequence to form the existing slope cutting and the third part of excavation the actual construction sequence to form the reinforced slope cutting.

The soil was assumed to be a nonlinear elastic material with a hyperbolic stress-strain relation and the soft rock a linear elastic. The slippage between the reinforcement and the surrounding medium was modeled by an elastoplastic joint element (Matsui and San, 1989 b). The reinforcement was considered as one dimensional bar element. The material properties used in the presnt analysis are summarized in Table 1. The cohesion and the internal friction angle of the soil were obtained from the back analysis of previous landslide occurred at the nearby area of the site. The hyperbolic parameters of the soil, such as K, R_f, n, were estimated from the standard penetration test results. The details of the evaluation of the material properties was reported elsewhere (Matsui and San, 1990 a).

Fig. 10 shows the axial force distributions of reinforcements at the stable condition after the completion of the excavation tests obtained from field measurements and the

Table 1. Material properties (Nose Study)

	Residual soil	Soft rock	Reinforcement
Elastic modulus E (MPa)	66.0	1.2×10^3	2.1×10^5
Unit weight γ (kNm^{-3})	18	20	—
Poisson's ratio ν	0.3	0.3	0.3
Friction angle ϕ (degree)	26.6	35	—
Cohesion c (kPa)	10.0	10.0	—
Coefficient of earth pressure at rest K_0	0.55	0.55	—
Hyperbolic constant K	900	—	—
Hyperbolic constant K_{ur}	1600	—	—
Hyperbolic constant n	1.02	—	—
Failure ratio R_f	0.69	—	—
Cross section area A (m^2)	—	—	3.8×10^{-4}

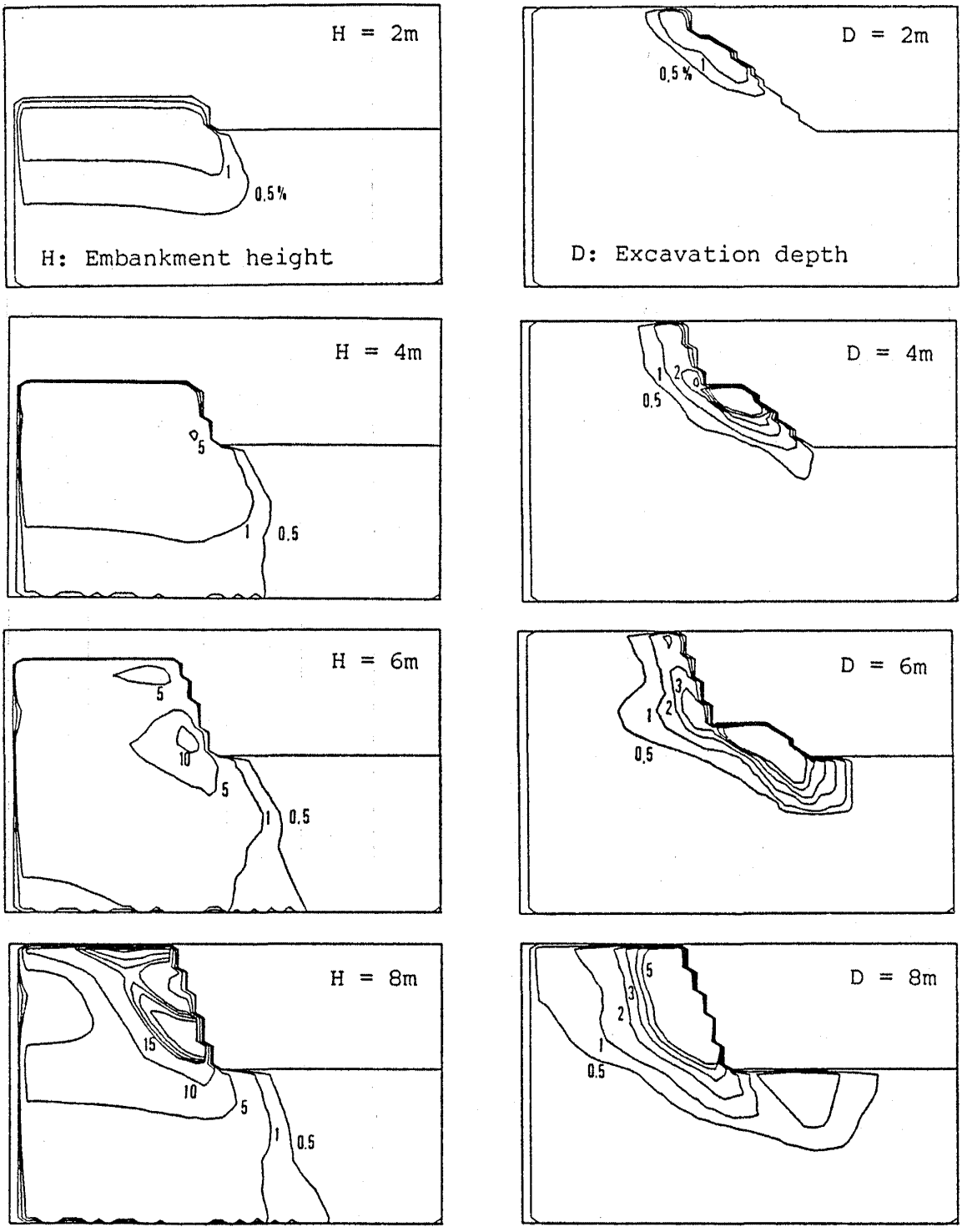

Fig. 7. Comparison between the development of total shear strain in the embankment slope and that of shear strain increment in the excavation slope during construction

analysis. Analytical results seem to approximately agree with the measured ones.

Fig. 11 shows the shear strain increment distribution of the existing slope for the cases of $R=1.0$ and $R_c=1.9$. The shear strain increment increases as the value of R in-

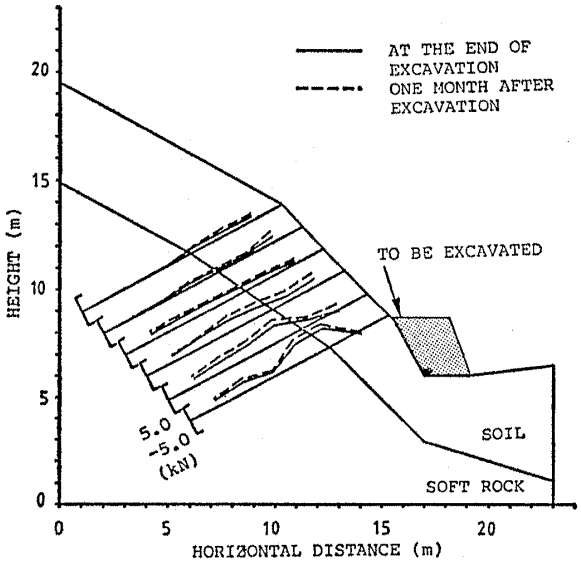

Fig. 8. Measured axial forces of the reinforcements

creases. Fig. 12 shows the failure patterns of the existing slope for the cases of $R=0.1$ and $R_c=1.9$. The dotted pattern shown in Fig. 12 represents the analytical data by the shear strength reduction technique, in which the shear strain increment exceeds 1%. The reason of the use 1% as failure shear strain increment will be discussed later. The failure slip surface of the existing slope by the Fellenius' method is also given in Fig. 12. The failure pattern of the existing slope by the proposed method agrees with that by the Fellenius' method.

The safety factor of the existing slope was then calculated from the local safety factor surface, which was constructed, being based on the local safety factors of all elements. The details of the use of the local safety factor surface to obtain the safety factor has been presented in our previous paper (Matsui and San, 1990 b). The safety factors of the slope obtained by the Fellenius' method and the proposed method are 1.21 and 1.28, respectively. It is demonstrated again that both the slip surface and safety factor by the proposed method are close to those by the Fellenius' method.

Fig. 13 shows the failure pattern of the reinforced slopes. The dotted area shown in Fig. 13 represents the analytical data by the

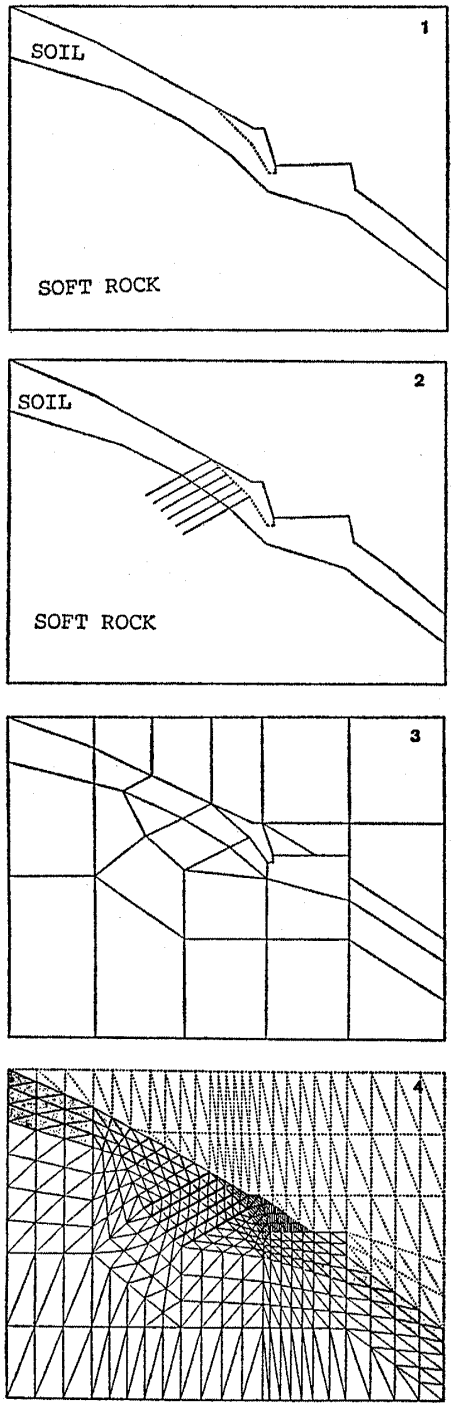

Fig. 9. Automatic mesh generation of the reinforced slope

shear strength reduction technique, in which the shear strain increment exceeds 1%. The failure firstly developed at the toe of the slope, such as shown in Fig. 13(a) for the case of $R=1.0$. The failure zone extended from the toe to the top of the slope as the value of R increases. A notable failure slip

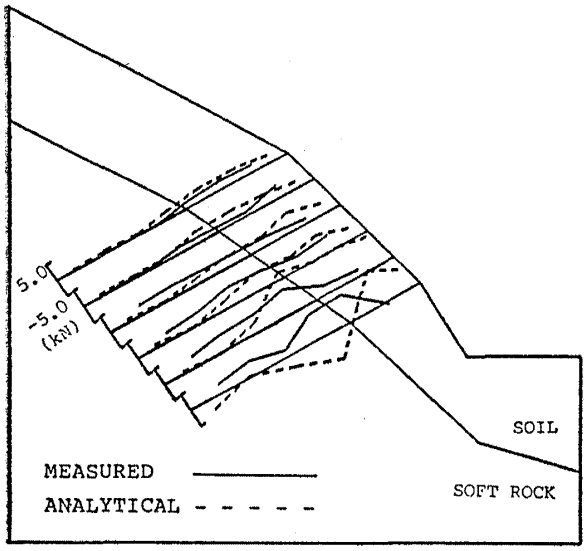

Fig. 10. Measured and analytical axial force distributions

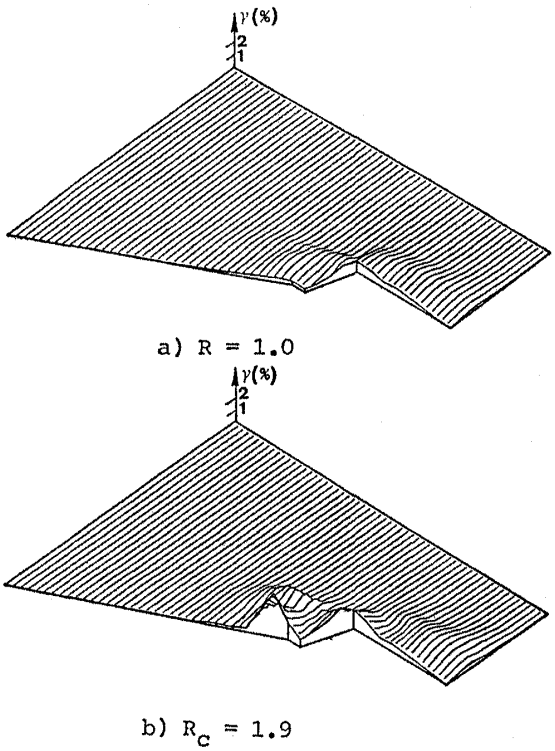

Fig. 11. Shear strain increment distributions of the existing slope with different values of *R*

surface was traced at R_c as shown in Fig. 13(b).

A minor failure of the reinforced slope occurred soon after the excavation. At that time the lower part of slope facing was not yet completed. The observed local failure

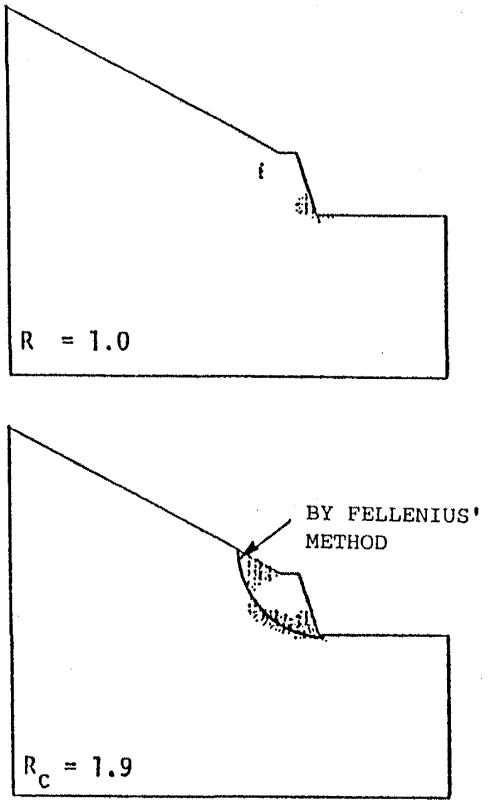

Fig. 12. Failure patterns of the existing slope with different values of *R*

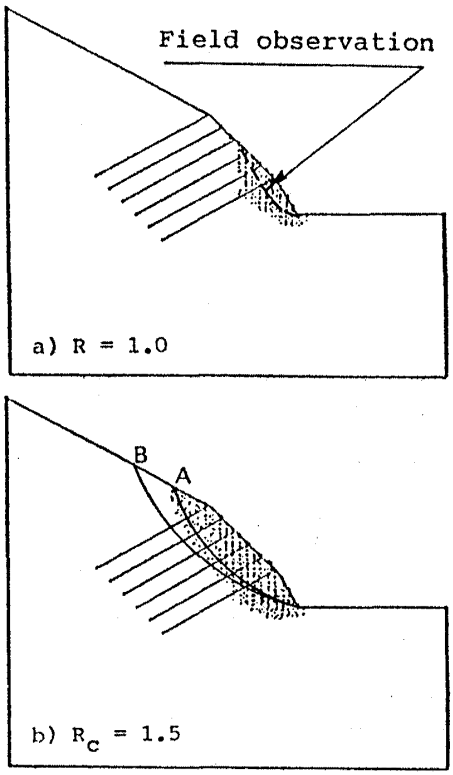

Fig. 13. Failure patterns of the reinforced slope with different values of *R*

slip surface is marked in the Fig. 13(a) for the comparison. The analytical result approximately agrees with the site observation. Based on the local safety factor, the safety factor along the minor failure slip surface was calculated to be 1.02.

As shown in Fig. 8, it can be seen that the axial forces developed in the lower three reinforcements were much larger than the upper ones at the time when the local failure occurred and the locations of the maximum tensile forces agree with the observed and predicted potential local failure slip surfaces shown in Fig. 13(a). The predicted potential overall failure slip surface, such as shown in Fig. 13(b), passes the locations of the maximum tensile forces measured at the stable condition after the completion of the excavation.

Based on the local safety factor surface and the slip surface traced by the shear strength reduction technique, the safety factor of the reinforced slope was calculated to be 1.12.

COMPARISON BETWEEN THE SHEAR STRENGTH REDUCTION TECHNIQUE AND A MODIFIED FELLENIUS' METHOD

Based on the strain compatibility between the soil and the reinforcement, a modified Fellenius' method for reinforced slope is proposed. It consists of such three steps as determining the failure slip surface of the reinforced slope, estimating the axial force of the reinforcement and calculating the safety factor of the reinforced slope.

In the limit equilibrium analysis, the safety factor F_S is defined as

$$F_S=\frac{F_r}{F_d} \qquad (3)$$

where F_r is the resistance foece, F_d the driving force.

In the Fellenius' method, F_r and F_d are given by

$$F_r=\Sigma\,(W\cos\alpha\tan\phi+cl) \qquad (4)$$

$$F_d=\Sigma W\sin\alpha \qquad (5)$$

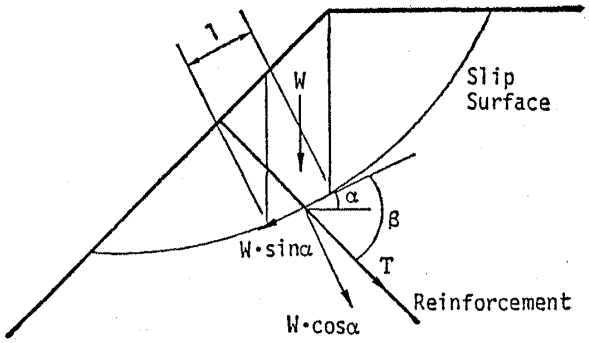

Fig. 14. Limit equilibrium method for the reinforced slope

where W is the weight, l the length of slip surface and α the angle of inclination of a slice, as shown in Fig. 14.

In slice method, by trying a large number of slip surfaces the most critical slip surface, i.e. the slip surface with the minimum safety factor, can be determined from Eq. (3).

The slope stability analysis of a reinforced slope may be facilitated by considering the out of balance force P for a certain required value of F_S, such as

$$P=F_S\times F_d-F_r \qquad (6)$$

The maximum out of balance force P_{max} can be determined from the slice method. In general, the value of F_S is specified in accordance with design criteria. But, in this paper, F_S is back analyzed from the measured tensile forces of the reinforcements. Consequently, the failure slip surface of the reinforced slope can be determined from Eq. (6).

Next, based on the strain compatibility between the soil and the reinforcement, the axial force developed in the reinforcement is estimated. As shown in Fig. 15, with the assumption that the development of strain in the reinforcements corresponds to that of the soil in its direction, the maximum shear strain increment $d\gamma_{max}$ along a slip surface can be calculated from the measured axial strain increment $d\varepsilon$ of the reinforcements by the following equation,

$$d\varepsilon=[\sin\Psi-\cos(\Psi-\theta)\sin\theta]d\gamma_{max} \qquad (7)$$

where Ψ is the dilatancy angle, θ the inclination of reinforcement to the normal of

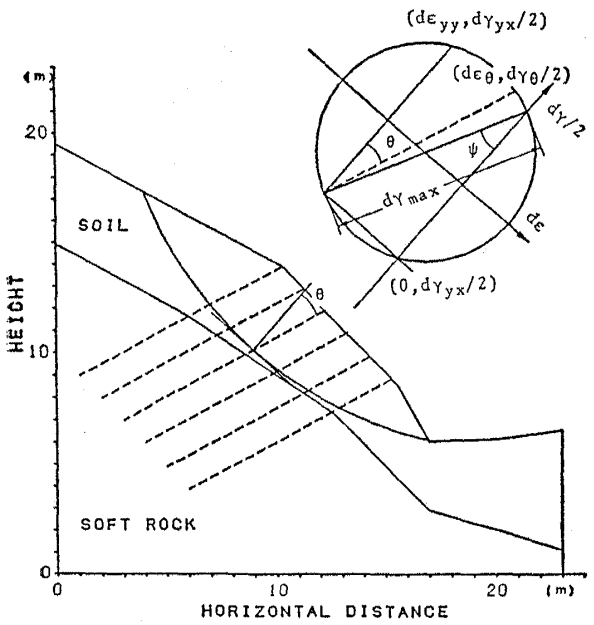

Fig. 15. Relationship of both strains developed in the reinforcement and in the soil

the slip surface.

From the axial strain the axial force of the reinforcement can be calculated, such as

$$T = E_R \times d\varepsilon \times A_R \qquad (8)$$

where E_R and A_R are the elastic modulus and cross-sectional area of the reinforcement.

It is assumed that the maximum out of balance force P_{max} is equal to the sum of the additional resistance force F_{radd} due to the reinforcements. F_{radd} can be determined from the axial force of the reinforcement T, such as

$$F_{radd} = T(\sin\beta \tan\phi + \cos\beta) \qquad (9)$$

where β is the intersection angle between the slip surface and the reinforcement, as shown in Fig. 14.

Then the safety factor of the reinforced slope can be estimated by

$$F_S = \frac{(F_r + \Sigma F_{radd})}{F_d} \qquad (10)$$

In the following, for the reinforced slope described in the previous chapter, the stability analysis result by the modified Fellenius' method is compared with that by the shear strength reduction method.

By using Eqs. (6), (9) and (10), together with the measured axial forces of the reinforcements, the safety factor of the reinforced slope was calculated to be 1.13, which is quite close to that from the shear strength reduction technique.

Also, if the associated flow rule is used, the dilatancy angle is 26.6°. Based on the measured axial forces of the reinforcements, the maximum shear strain of the soil is estimated to be about 0.5% (Matsui, San and Hayashi, 1990). The slippage between the reinforcement and the soil is not included in Eq. (7), therefore, the failure shear strain increment is assumed as 1% in the stability analysis by the shear strength reduction technique, as described in the previous chapter.

The slip surfaces A and B, as shown in Fig. 13(b), are the potential failure slip surfaces with the minimum safety factor F_{Smin} and with the maximum out of balance force P_{max}, respectively. The slip surface A corresponds to the critical slip surface for the unreinforced slope. The slip surface with P_{max} moves a bit far away from the surface of the slope by comparing with that with F_{Smin}. The slip surface with P_{max} is a little bit closer to the locations of the measured maximum tensile forces of the reinforcements. The failure slip surface by the shear strength reduction technique locates in the middle part between the slip surfaces, A and B.

CONCLUSIONS

In this paper, verification of the shear strength reduction technique to finite element slope stability analysis was presented. Availability of the shear strength reduction technique for both embankment and excavation slopes was illustrated. Applicability of the proposed method to practical reinforced slope cutting design works was examined through the field test data and the comparison with a modified Fellenius' method.

The analytical results demonstrated that the slip surface can be successfully traced for both embankment and excavation slopes by the shear strength reduction technique.

The physical meaning of the critical shear strength reduction ratio was elucidated in regard to the total shear strain and shear strain increment for both embankment and excavation slopes. The predicted failure slip surface of the reinforced slope cutting agreed with the field test data and site observation. Agreement between the shear strength reduction technique and the modified Fellenius' method was satisfactory.

As the results, the potential of the use of the proposed method to practical design works was demonstrated.

REFERENCES

1) Duncan, J. M. and Chang, C. Y. (1970) : "Nonlinear analysis of stress and strain in soils," J. Soil Mech. and Found. Engg. Div., ASCE, Vol. 96, No. SM 5, pp. 1629-1653.
2) Matsui, T. and San, K. C. (1988) : "Finite element stability analysis method for reinforced slope cutting," Proc. International Geotechnical Symposium on Theory and Practice of Earth Reinforcement, Fukuoka, pp. 317-322.
3) Matsui, T. and San, K. C. (1989 a) : "Verification of the analysis method for reinforced slopes," Proc. 12 th International Conference on SMFE, Brazil, Vol. 2, pp. 1277-1280.
4) Matsui, T. and San, K. C. (1989 b) : "An elastoplastic joint element with its application to reinforced slope cutting," Soils and Foundations, Vol. 29, No. 3, pp. 95-104.
5) Matsui, T. and San, K. C. (1990 a) : "Design method for reinforced slope of residual soil," Proc. 10 th Southeast Asian Geotechnical Conference, Taipei, Vol. 1, pp. 101-106.
6) Matsui, T. and San, K. C. (1990 b) : "A hybrid slope stability analysis method with its application to reinforced slope cutting," Soils and Foundations, Vol. 30, No. 2, pp. 79-82.
7) Matsui, T. San, K. C. and Hayashi, K. (1990) : "Design and field test on a reinforced cut slope," Proc. International Reinforced Soil Conference, Glasgow, pp. 235-240.
8) Roscoe, K. H. (1970) : "The influence of strains in soil mechanics, Tenth Rankine Lecture," Geotechnique Vol. 20. No. 2, pp. 129-170.
9) San, K. C., Matsui, T. and Katsuraya, R. (1990) : "Some aspect of the slope stability analysis by shear strength reduction technique," Proc. Symposium on Geology and Slope Failure, JSSMFE: pp. 43-48 (in Japanese).
10) San, K. C. and Matsui, T. (1991) : "Finite element slope failure prediction by shear strength reduction technique," Proc. International Symposium on Natural Disaster Reduction and Civil Engineering, JSCE., Osaka, pp. 359-366.
11) Ugai, K. (1990) : "Availability of shear strength reduction method in stability analysis," Tsuchi-to-Kiso, Vol. 38, No. 1, pp. 67-72 (in Japanese).